ACS APPLIED MATERIALS & INTERFACES

Research Article

www.acsami.org

Single-Crystalline Nanogap Electrodes: Enhancing the Nanowire-Breakdown Process with a Gaseous Environment

Hiroshi Suga,*[,†] Touru Sumiya,[‡] Shigeo Furuta,[‡] Ryuichi Ueki,[§] Yosuke Miyazawa,[§] Takuya Nishijima,[§] Jun-ichi Fujita,[§] Kazuhito Tsukagoshi,[⊥] Tetsuo Shimizu,[#] and Yasuhisa Naitoh*[,#]

[†]Department of Mechanical Science and Engineering of Chiba Institute of Technology, 2-17-1 Tsudanuma, Narashino, Chiba 275-0016, Japan

[‡]Funai Electric Advanced Applied Technology Research Institute Inc., TCI A37, 2-1-6 Sengen, Tsukuba, Ibaraki 305-0023, Japan

[§]Institute of Applied Physics, University of Tsukuba, Tennoudai 1-1-1, Tsukuba, Ibaraki 305-8573, Japan

[⊥]National Institute for Materials Science (NIMS), Namiki 1-1, Tsukuba, Ibaraki 305-0044, Japan

[#]National Institute of Advanced Industrial Science and Technology (AIST), Higashi 1-1-1 Tsukuba, Ibaraki 305-8562, Japan

Supporting Information

ABSTRACT: A method for fabricating single-crystalline nanogaps on Si substrates was developed. Polycrystalline Pt nanowires on Si substrates were broken down by current flow under various gaseous environments. The crystal structure of the nanogap electrode was evaluated using scanning electron microscopy and transmission electron microscopy. Nanogap electrodes sandwiched between Pt-large-crystal-grains were obtained by the breakdown of the wire in an O_2 or H_2 atmosphere. These nanogap electrodes show intense spots in the electron diffraction pattern. The diffraction pattern corresponds to Pt (111), indicating that single-crystal grains are grown by the electrical wire breakdown process in an O_2 or H_2 atmosphere. The Pt wires that have (111)-texture and coherent boundaries can be considered ideal as interconnectors for single molecular electronics. The simple method for fabrication of a single-crystalline nanogap is one of the first steps toward standard nanogap electrodes for single molecular instruments and opens the door to future research on physical phenomena in nanospaces.

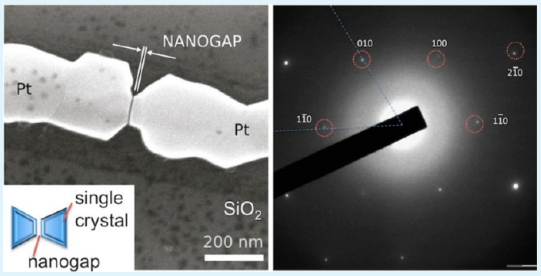

KEYWORDS: *nanogap, electro migration, single molecule electronics, single crystal, break junction, platinum*

INTRODUCTION

Recent interest in nanoscale devices and single-molecule electronics has spurred interest in design strategies for nanogap electrodes.[1,2] Nanoparticles or molecules confined in nanogaps can perform functions similar to those of transistors or sensors.[3,4] Nanogaps (without nanomaterials) exhibit various phenomena such as surface plasmon enhancement and giant magnetoresistance.[5,6] These phenomena are sensitive to nanogap size and shape. A number of strategies that employ mechanical break junctions (MBJs), electron-beam lithography, or chemical etching[7−9] have been developed to design nanogap electrodes.

To date, however, no efforts have been made to control the crystal structure of the electrodes. Disorder in the crystal structure causes instabilities in nanogap characteristics. For example, as electron transport depends on the work function and because different crystal planes in a material have varying work functions,[10] unstable electron transport occurs in electrodes composed of polycrystalline surfaces. Here, we fabricate a nanogap sandwiched between two single crystals as a first step toward the design of a standard nanogap for single molecular instruments or nanogap devices.

We combined two established methods, one for metal−surface reconstruction using flame annealing and cooling in gas atmospheres, and another for creating polycrystalline nanogap electrodes from polycrystalline nanowires on Si substrates.[11−14] We developed this novel method for fabricating single-crystalline nanogaps from polycrystalline Pt nanowires on Si substrates using electrical wire break junction processes in gaseous environments. Conditions of the gas species, pressure were established. After fabrication, the electrodes were evaluated using a scanning electron microscope (SEM) and electron diffraction analysis of transmission electron microscope (TEM). As a result, a nanogap was formed between large-grain-boundaries upon the introduction of the Oxygen (O_2) gas or hydrogen (H_2) gas. Those nanogap electrodes have the intense spots of electron diffraction analysis of TEM. These diffraction patterns correspond to diffraction spot of Pt (111), which means the single-crystal grains grew by electrical break junction process in the O_2 or H_2 ambient. The Pt wires which have the (111)-texture and coherent boundaries can be

Received: July 24, 2012
Accepted: September 25, 2012
Published: October 10, 2012

considered ideal for interconnects for single molecular electronics. Single-crystalline nanogap electrodes can be fabricated easily using this method. Fabrication of this single-crystalline nanogap opens the door to future research in nanospace and nanomaterials in nanospace.

EXPERIMENTAL SECTION

Nanogap electrodes were constructed from polycrystalline Pt nanowires. The nanowires were fabricated on a SiO_2 layer of a 300-nm-thick Si substrate. Nanowires with widths of 400 nm and lengths of 5 μm were patterned using high-resolution electron beam lithography. After the resist patterning, a 5-nm-thick Cr thin film and a 30-nm-thick Pt thin film were deposited by vacuum evaporation. After lift-off of the resist, Au pads for electrical connections were deposited at both ends of the Pt nanowire.

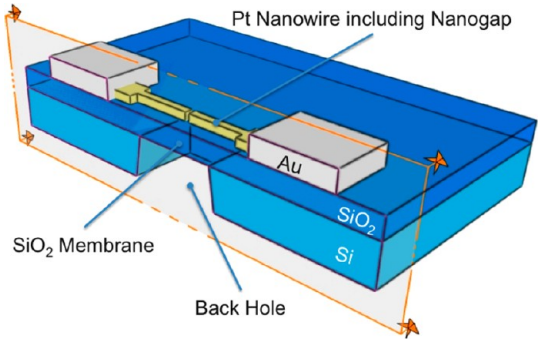

Figure 1. Schematic diagram of a nanogap electrode on a transparent SiO_2 membrane. The orange box outlines the cross-section. The Pt nanowire and nanogap form above a SiO_2 membrane. A SiO_2 hole is etched out of the Si/SiO_2 wafers. The white blocks represent the gold pads used for the electrical connection.

The nanogaps were formed in a closed chamber equipped with a gas inlet valve. The Pt polycrystalline nanowire was broken down by current flow. The electrical break junction process was performed under controlled gas conditions. In this study, six conditions were examined: in vacuum ($<1 \times 10^{-4}$ Pa) under oxygen (O_2) gas, under nitrogen (N_2) gas, under argon (Ar) gas, under Ar gas containing 4% hydrogen (H_2), and in dry air. The voltages applied to the nanowire were controlled using previously reported procedures.[14] The voltages were increased in 10 mV steps and the current was monitored with a sourcemeter (Keithley 2636, USA). When the resistance of the nanowires changed drastically, the applied voltage was returned to 0 V immediately and then increased. The Joule heating and the use of intermittent voltages mimic the processes of flame annealing and cooling. When the $I-V$ curve deviated from metallic conduction behavior (i.e., exhibited close to tunnel conduction behavior),[14] the procedure was terminated.

The shape and morphology of the nanogap electrodes were observed using scanning electron microscopy (SEM, Hitachi S4500, Japan). The crystal structures of the nanogap electrodes were identified from the electron diffraction patterns obtained from transmission electron microscopy (TEM, JEOL JEM2100, Japan) images. The TEM images, confirmed that polycrystalline Pt nanogap electrodes on transparent SiO_2 membrane were fabricated.[15,16] Figure 1 shows the schematic diagram of the nanogap electrode on a transparent SiO_2 membrane. The membrane consisted of 50×50 μm^2 SiO_2 (100 nm thick) layer etched out of Si/SiO_2 wafers (Figure 1).

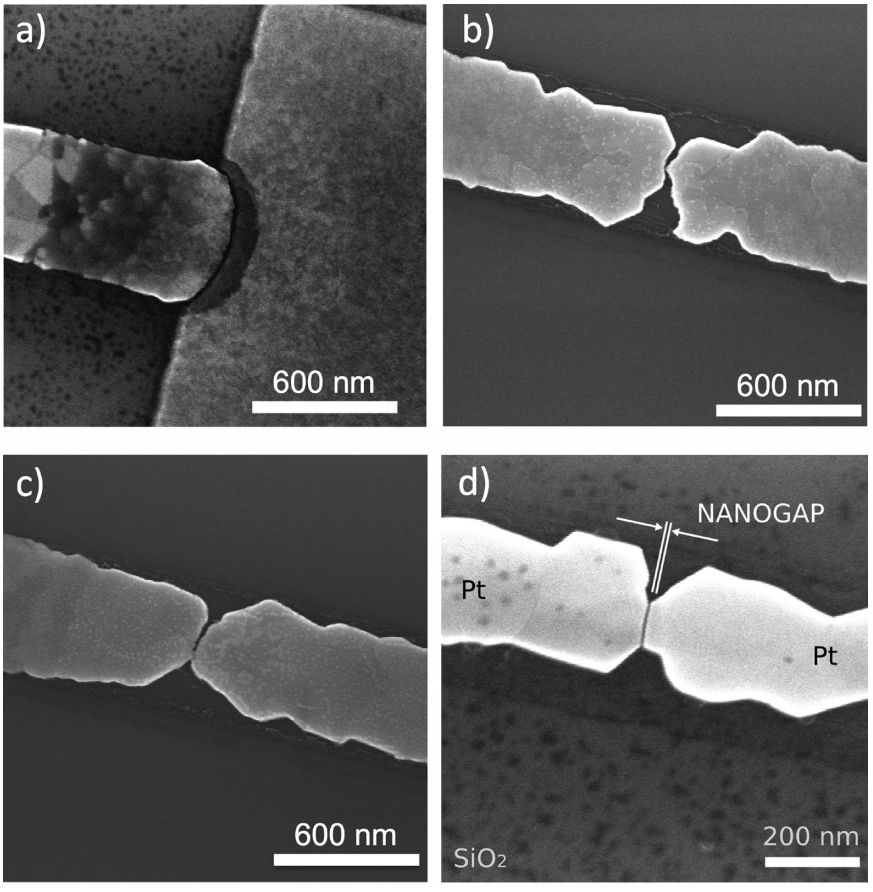

Figure 2. SEM images of nanogap electrodes on a SiO_2 substrate. The nanogaps were fabricated in (a) vacuum, (b) dry air, (c) N_2, and (d) O_2.

dx.doi.org/10.1021/am301441a | ACS Appl. Mater. Interfaces 2012, 4, 5542−5546

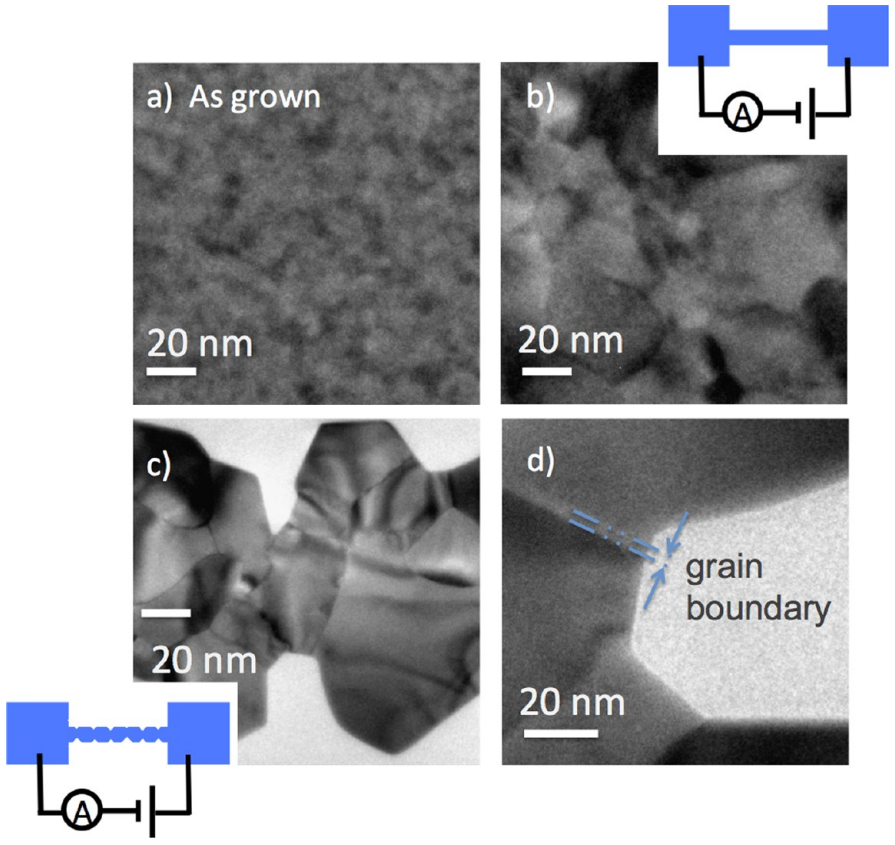

Figure 3. (a) TEM image of the electrode as-grown surface. (b–d) Changes in the surface morphology with applied current. Insets in b and d: schematic diagrams illustrating the gap formation sequence, and the arrows in d mark the grain boundary.

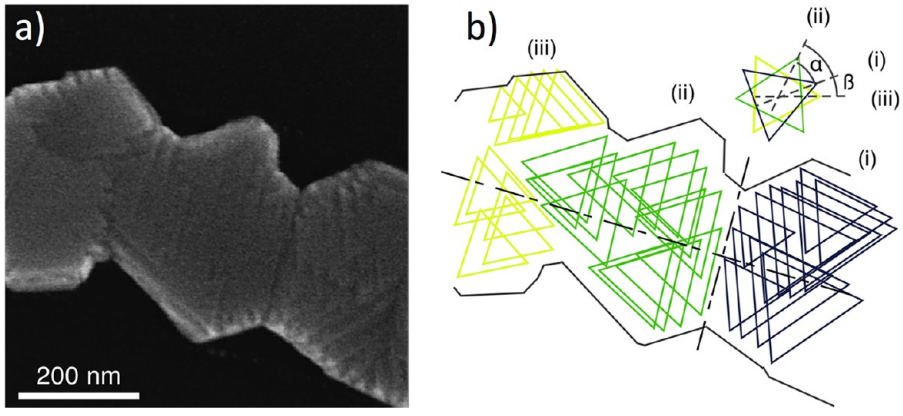

Figure 4. (a) SEM micrograph of a nanowire just prior to breaking. (b) Plot of triangle grains in the boundary.

RESULTS & DISCUSSION

Figure 2 shows the SEM images of the nanogap electrodes fabricated under different atmospheric conditions. The nanogap in Figure 2a was formed in a 1.0×10^{-5} Pa vacuum. The surfaces around the nanogap consist of polycrystalline Pt. The nanogap in Figure 2b was obtained in dry air at 2.0×10^{4} Pa. Facets of the Pt crystal were observed around the nanogap. This indicates that dry air assists facet growth. However, the nanogap in Figure 2b does not consist of a single-crystal surface. The nanogaps shown in images c and d in Figure 2 were obtained under N_2 and O_2 atmospheres, respectively, at 2.0×10^{4} Pa. The nanogap obtained in the O_2 atmosphere is the object of this study. From Figure 2d, we observe that the crystal size of the Pt nanowires is different from the as-grown Pt thin film. A nanogap was formed between the two crystal facets. The gap width was normalized by the width of the grain boundary, and the gap length was normalized by the length of a facet of the crystal grain. The gap width and length were 2 and 100 nm, respectively, as shown in the SEM image. To the best of our knowledge, such high-aspect nanogaps have not been reported.[1,2] In the future, improvements in crystal growth techniques may allow the fabrication of nanogaps of arbitrary dimensions. These results indicate that a highly crystalline nanogap electrode was fabricated by the electrical Pt wire breakdown in O_2.

The sequence of gap formation is elucidated by the SEM images of the surface of the nanowire prior to electrical wire breakdown. Figure 3 shows the TEM image of the nanowire on

dx.doi.org/10.1021/am301441a | ACS Appl. Mater. Interfaces 2012, 4, 5542–5546

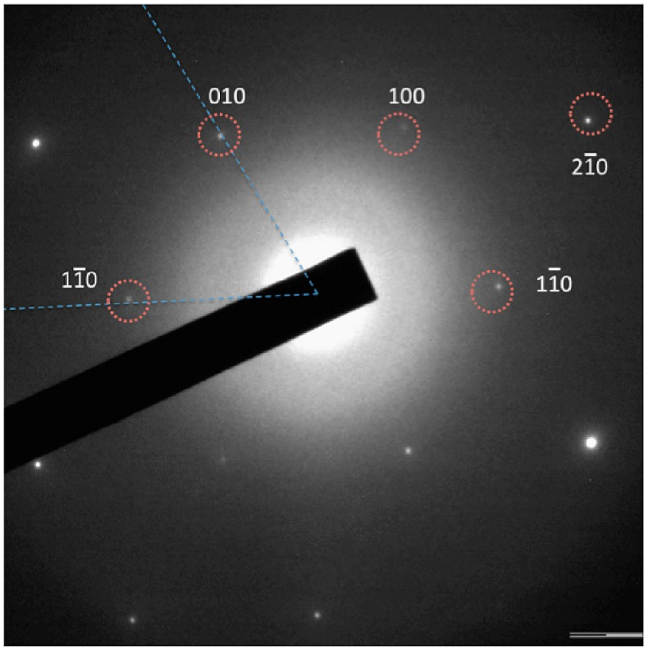

Figure 5. Electron beam diffraction analysis of the area on the nanogap electrodes. The intense spots indicate that the top-facing surface is Pt (111).

a SiO_2 membrane. In Figure 3a there is no current flow (as-grown sample), and the polycrystalline surface is observed. When a current is applied to the polycrystalline nanowire, Joule heating, electromigration, and gas diffusion all promote crystal growth in the nanowire (Figure 3b). The crystal grains formed a deep groove at the grain boundary, as shown Figure 3c. Previous studies found that atoms at the grain boundary migrate easily during the final stages of feedback break-junction.[17,18] The diffusion energy of Pt atoms at the grain boundary is lower than the diffusion energy of the atoms in the grain.[19] These results imply that atoms in the grain boundary migrate leaving a nanogap. When the single crystal grain size was larger than the nanowire width, the Pt atoms at the grain boundary were removed, as shown in Figure 3d. Figure 4a is the SEM image of the nanowire just prior to breaking. Triangular grains on the wire were observed, indicating that crystal growth was completed before the break occurred. Figure 4b is a plot of the boundary shape. Three types of triangles that have different angles to the axis of the nanowire are observed. Similar shaped triangles form hexagonal grains and grain boundaries form between the different triangular-shaped grains. Triangle (i) is tilted 44° to form triangle (ii), and triangle (iii) is tilted 61.7° to form triangle (ii).

The crystal structure of the nanogap electrode fabricated in an O_2 atmosphere was evaluated. Figure 5 shows the transmission electron diffraction pattern taken from a selected area (spotsize is 150 nm in diameter) on the nanogap electrodes. As shown in Figure 5, the intense spots are from Pt on the amorphous SiO_2 layer. From the direction of the diffraction spots from Pt (111),[20] it is reasonable to assume that the top-facing surface of the nanogap electrode is Pt (111). We conclude that single-crystal grains are grown by electrical wire breakdown processes in an O_2 atmosphere.

To understand the effect of gases on nanogap formation, we fabricated a nanogap in Ar atmosphere. Generally, single-crystal growth on metal surfaces occurs under heating and cooling conditions. The thermal conduction rate is a key parameter of gas cooling. The thermal conduction rates of N_2, O_2, and Ar are 25.9, 26.4, and 17.8 mW m^{-1} K^{-1}, respectively, at 300 K and 1 atm.[21] Figures 6a, 2c, and 2d show images of the nanogap electrode fabricated under Ar, N_2, and O_2 atmospheres, respectively. The fabrications performed in Ar, N_2, and O_2 do not correspond to their respective thermal conduction rates. To investigate the effects of gas adsorption and reaction on Pt surfaces, we added a small amount of H_2 gas. Figure 6b shows a nanogap fabricated under an Ar atmosphere containing 4% H_2. The 4% H_2 gas led to unambiguous crystal growth. Gas adsorption and reaction on Pt surface play a role in this fabrication method. Gas species that react with platinum are the basis of this method. The single-crystal electrode was fabricated under pressures of 1.0×10^3 Pa to 1.4×10^5 Pa (the upper limit is the maximum pressure that can be obtained in our vacuum chamber). We can fabricate single-crystalline nanogaps using simple procedures without adjusting gas pressure precisely. (More Examples of nanogap electrodes were shown in Figure S1 in the Supporting Information.) Here, the gas adsorption and reaction on Pt surfaces are discussed. Atoms are adsorbed during the electromigration process over stable atomic planes. A previous study that used this feedback electromigration process,[22] was unsuccessful in growing large crystal grains. Using our method, however, we are able grow large crystals

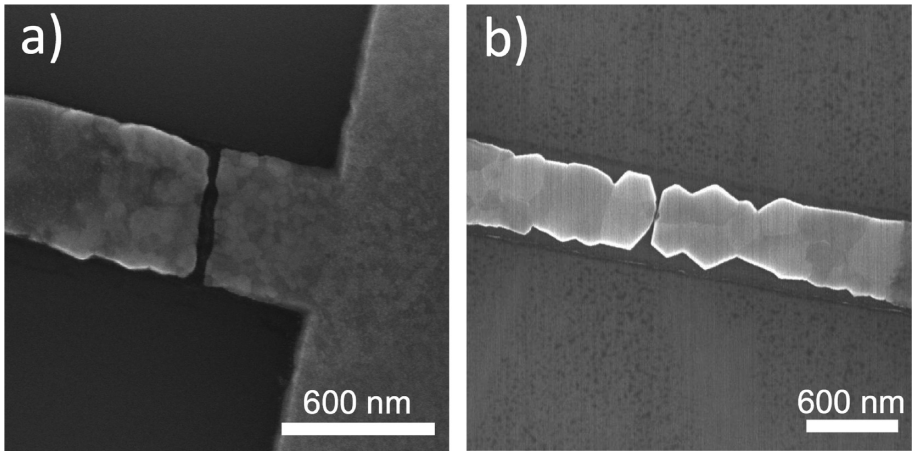

Figure 6. SEM micrograph of nanogap electrodes formed in (a) Ar atmosphere and (b) Ar atmosphere containing 4% H_2.

using feedback electromigration. It is well-known that chemisorption of H_2 and O_2 occurs in Pt catalysis.[23] The dissociative chemisorption of H_2 and O_2 shows a strong selectivity for the crystal plane,[24,25] and reduces the Pt−Pt binding energy.[26,27] The effect of the gas is to increase the surface energy difference between a specific crystal plane and other planes. In the feedback electromigration process, the voltages for adatom migrations vary depending on the crystal plane.[17,28] Therefore, adatoms on specific atomic planes preferentially migrate during the process. It can be expected that the dissociative chemisorption of H_2 and O_2 makes specific crystal structure friable and promotes the growth of different crystal structures. Large crystal grains and sharp facets were generated in all nanowires. Atoms in the grain boundary are removed by electromigration, resulting in nanogap formation. As the diffusion energy of atoms in the crystal structure increase with growth of the crystal-grain-size, sharp-edged nanogap electrodes form at grain boundaries and are sandwiched between highly crystalline regions.

CONCLUSION

A nanospace sandwiched between two single crystals was obtained. A novel method for fabricating single-crystal nanogap electrodes from polycrystalline Pt nanowires on Si substrates was developed. The method employs electrical breakjunction in O_2 or H_2 ambient. A nanogap sandwiched between Pt (111) grains was fabricated. The gas species contribute to single-crystal growth. Single-crystal nanogap can be fabricated easily using this method. Single-crystalline nanogaps open the door to future research on physical phenomena in nanospaces.

ASSOCIATED CONTENT

Supporting Information

SEM images of nanogap electrodes fabricated under O_2 and H_2 atmospheres. This material is available free of charge via the Internet at http://pubs.acs.org/.

AUTHOR INFORMATION

Corresponding Author

*E-mail: hiroshi.suga@it-chiba.ac.jp (H.S.); ys-naitou@aist.go.jp (Y.N.). Phone: +81-47-478-0507 (H.S.); +81-29-861-7892 (Y.N.).

Notes

The authors declare no competing financial interest.

ACKNOWLEDGMENTS

The authors extend their deep appreciation to Mr. Y. Masuda, Mr. T. Takahashi, and Dr. M. Ono of Funai Electronics Advance Applied Technology Research Institute, Inc., and Ms. M. Horikawa of AIST for their advice on a wide range of issues regarding this work. The sample fabrication was partly supported by the Nanotechnology Innovation Center Nano-Integration Facility in NIMS and Keithley Instruments, Inc. This research was supported by a Grant-in-Aid for Scientific Research (23760320) from the Japan Society for the Promotion of Science.

REFERENCES

(1) Li, T.; Hu, W.; Zhu, D. *Adv. Mater.* **2010**, *22*, 286−300.
(2) Tian, X.; Li, J.; Xu, D. *Electrochem. Commun.* **2010**, *12*, 1081−1083.
(3) Reed, M. A.; Zhou, C.; Muller, C. J.; Burgin, T. P.; Tour, J. M. *Science* **1997**, *278*, 252−254.
(4) Bezryadin, A.; Dekker, C.; Schmid, G. *Appl. Phys. Lett.* **1997**, *71*, 1273−1275.
(5) Pile, D. F. P.; Ogawa, T.; Gramotnev, D. K.; Matsuzaki, Y.; Vernon, K. C.; Yamaguchi, K.; Okamoto, T.; Haraguchi, M.; Fukui, M. *Appl. Phys. Lett.* **2005**, *87*, 261114−1−3.
(6) Cespedes, O.; Watts, S. M.; Coey, J. M. D.; Dorr, K.; Ziese, M. *Appl. Phys. Lett.* **2005**, *87*, 083102−1−3.
(7) Moreland, J.; Ekin, J. W. *J. Appl. Phys.* **1985**, *58*, 3888−3895.
(8) Sutanto, J.; Smith, R. L.; Collins, S. D. *J. Micromech. Microeng* **2010**, *20*, 045016−1−7.
(9) Guillorn, M. A.; Carr, D. W.; Tiberio, R. C.; Greenbaum, E.; Simpson, M. L. *J. Vac. Sci. Technol. B* **2000**, *18*, 1177−1181.
(10) Sargood, A. J.; Jowett, C. W.; Hopkins, B. J. *Surf. Sci.* **1970**, *22*, 343−356.
(11) Clavilier, J.; Faure, R.; Guinet, G.; Durand, R. *J. Electroanal. Chem.* **1980**, *107*, 205−209.
(12) Markovic, N.; Hanson, M.; Mcdougall, G.; Yeager, E. *J. Electroanal. Chem.* **1986**, *214*, 555−566.
(13) Kibler, L. A.; Cuesta, A.; Kleinert, M.; Kolb, D. M. *J. Electroanal. Chem.* **2000**, *484*, 73−82.
(14) Strachan, D. R.; Smith, D. E.; Johnston, D. E.; Park, T.-H.; Therien, M. J.; Bonnell, D. A.; Johnson, A. T. *Appl. Phys. Lett.* **2005**, *86*, 043109−1−3.
(15) Kanaya, K.; Okayama, S. *J. Phys. D* **1972**, *5*, 43−58.
(16) Strachan, D. R.; Smith, D. E.; Fischbein, M. D.; Johnston, D. E.; Guiton, B. S.; Drndić, M.; Bonnell, D. A.; Johnson, A. T. *Nano Lett.* **2006**, *6*, 441−444.
(17) Umeno, A.; Hirakawa, K *Appl. Phys. Lett.* **2009**, *94*, 162103−1−3.
(18) Umeno, A.; Hirakawa, K. *Physica E* **2010**, *42*, 2826−2829.
(19) Bassett, D. W.; Webber, P. R. *Surf. Sci.* **1978**, *70*, 520−531.
(20) Cowley, J. M. *Diffraction Physics*, 2nd ed.; North-Holland: Amsterdam, 1984.
(21) Lemmon, E. W.; Jacobsen, R. T. *Int. J. Thermophys.* **2004**, *25*, 21−69.
(22) Strachan, D. R.; Johnston, D. E.; Guiton, B. S.; Datta, S. S.; Davies, P. K.; Bonnell, D. A.; Johnson, A. T. C. *Phys. Rev. Lett.* **2008**, *100*, 056805−1−4.
(23) Masel, R. I. *Principles of Adsorption and Reaction on Solid Surfaces*; Wiley-Interscience: New York, 1996.
(24) Yotsuhashi, S.; Yamada, Y.; Kishi, T.; Diño, W.; Nakanishi, H.; Kasai, H. *Phys. Rev. B* **2008**, *77*, 115413−1−6.
(25) Ogasawara, H.; Ito, M. *Chemi. Phys. Lett.* **2000**, *221*, 213−218.
(26) Pauly, F.; Dreher, M.; Viljas, J.; Häfner, M.; Cuevas, J.; Nielaba, P. *Phys. Rev. B* **2006**, *74*, 235106−1−21.
(27) Untiedt, C.; Dekker, D.; Djukic, D.; Ruitenbeek, J. V. *Phys. Rev. B* **2004**, *69*, 081401.
(28) Nam, S. W.; Chung, H. S.; Lo, Y. C.; Qi, L.; Li, J.; Lu, Y.; Johnson, A. T. C.; Jung, Y.; Nukala, P.; Agarwal, R. *Science* **2012**, *336*, 1561−1566.